

Fluctuation Analysis of Rotational Decay from Excited Nuclei

B. Herskind,⁽¹⁾ A. Bracco,^{(2),(3)} R. A. Broglia,^{(1),(2),(3)} T. Døssing,⁽¹⁾ A. Ikeda,⁽⁴⁾ S. Leoni,^{(2),(3)}
J. Lisle,⁽⁵⁾ M. Matsuo,⁽⁶⁾ and E. Vigezzi⁽³⁾

⁽¹⁾*The Niels Bohr Institute, University of Copenhagen, DK-2100 Copenhagen, Denmark*

⁽²⁾*Dipartimento di Fisica, Università di Milano, 20133 Milano, Italy*

⁽³⁾*Istituto Nazionale di Fisica Nucleare, Sezione di Milano, 20133 Milano, Italy*

⁽⁴⁾*Shizuoka Institute of Science and Technology, Fukuori, Shizuoka 437, Japan*

⁽⁵⁾*Schuster Laboratory, University of Manchester, Manchester, United Kingdom*

⁽⁶⁾*Yukawa Institute, Kyoto, Japan*

(Received 5 February 1992)

A statistical method to analyze the gamma decay of excited, rapidly rotating nuclei is presented. It is based on the fact that the cooling path of these systems goes through regions of both suppressed and enhanced fluctuations typical of large and low level density, respectively. The method is applied to the study of the high-spin quasicontinuum of $^{167,168}\text{Yb}$.

PACS numbers: 24.60.Ky, 21.10.Re, 23.20.Lv, 27.70.+q

Nucleons can organize their motion in nuclei, leading to quadrupole deformed shapes of the average field. These nuclei can be produced at finite excitation energies and large angular momenta in fusion reactions induced by heavy-ion collisions. The resulting system cools down by particle and photon emission.

The associated continuum γ spectrum is mostly composed of stretched $E2$ transitions typical of rotational spectra. However, the correlation in the energy of two successive γ transitions is much weaker than that associated with the decay of a perfect rotor. For rotational bands, two transitions cannot have the same energy, whereas the experimental two-dimensional coincidence spectrum only displays a shallow valley running along the diagonal at $E_{\gamma_1} = E_{\gamma_2}$.

This observed deviation from the regular pattern is probably caused by the fact that the dominant part of the enhanced electric quadrupole decay passes through regions of high level density, where rotational bands become mixed, with mixing coefficients which change as a function of the spin. As a consequence, the $E2$ decay from a state of spin I will not go to a single state of spin $I-2$, but to a range of states [1-5], implying damping of the rotational motion. These transitions can be correlated with the intensities observed in the valleys, while the ridges are built out of discrete electric quadrupole transitions between states belonging to rotational bands close to the yrast line (cf. Fig. 1). Even if this picture seems to be fairly well established, central questions still remain to be answered: (i) How many levels are associated with the decay in the damped region, and how many in the case when the decay proceeds along discrete bands? (ii) What is the excitation energy above the yrast line which defines the onset of rotational damped motion, and to what extent is this a sharp transition? (iii) What is the shape of the strength function associated with the stretched quadrupole decay in the damped region?

The subject of the present paper is to study how these

two decay regimes manifest themselves in the fluctuations of the counting rate recorded in the experimental channels. The potential information contained in these fluctuations was first discussed in Ref. [6], and various aspects of the method have been presented in Refs. [7-9]. An excellent review of the statistical methods applied to nuclear single spectra can be found in Ref. [10].

There will be a certain probability for three given states at energies E_I , E_{I-2} , and E_{I-4} and angular momenta I , $I-2$, and $I-4$ to be connected by two consecutive γ transitions of energy $E_{\gamma_1} = E_I - E_{I-2}$, $E_{\gamma_2} = E_{I-2} - E_{I-4}$. When these two transitions are recorded by the detectors, a new count is added to the experimental two-dimensional spectrum of γ - γ coincidences. The two tran-

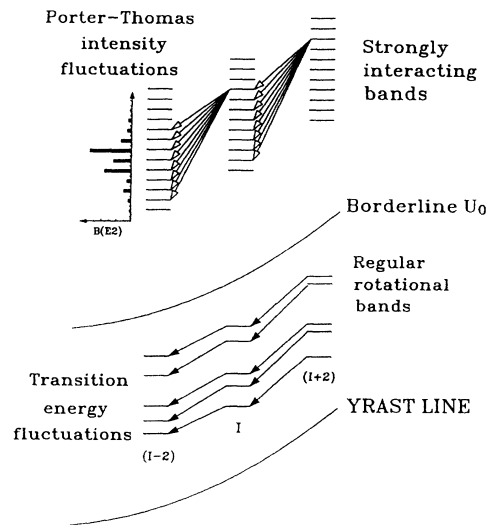


FIG. 1. Schematic representation of the γ -decay pattern of excited, rapidly rotating nuclei in the plane of excitation energy and spin.

sition energies E_{γ_1} and E_{γ_2} define a path i , which can be followed during the nuclear decay, with a probability W_i .

The average energy difference between two consecutive rotational transitions is equal to $8A$, where $A = \hbar^2/2J^{(2)}$ determines the energy scale of the rotational states, $J^{(2)}$ being the moment of inertia. Each cascade contributes, on average, one path to every $8A \times 8A$ two-dimensional energy interval. This energy window is divided into about 10^2 channels.

By selecting 2D energy intervals close to the valley diagonal, the most relevant information for the present discussion will be accumulated. That is, information concerning consecutive transitions in a discrete rotational band, or concerning two consecutive damped rotational transitions of energies close to the average. The rest of the paths, especially false paths with Compton transitions, will form a background which can be taken care of by background-reducing procedures, and well-determined correction factors.

For a path of energy $E_i \equiv (E_{\gamma_1}, E_{\gamma_2})$, there is a certain probability $P_j(E_i)$ for detection in a channel j , the result of the product of two one-dimensional probabilities for detecting each transition [$P_j(E_i) = p_{j_1}(E_{\gamma_1})p_{j_2}(E_{\gamma_2})$]. The total probability Q_j for an event to be recorded in channel number j is found by summing up over paths:

$$Q_j = \sum_{i=1}^{N_{\text{path}}} W_i P_j(E_i). \quad (1)$$

For a given number of recorded events N_{eve} , the probability distribution for detecting M_j events in channel j is binomial, governed by the probability Q_j for saying "yes" to channel j , and the probability $1 - Q_j$ for saying "no." Denoting the number of channels by N_{ch} , the first moment of the spectrum is given by $\mu_1 = N_{\text{eve}}/N_{\text{ch}}$.

The second central moment of this distribution is expressed through the path energies and probabilities:

$$\begin{aligned} \mu_2 &= \frac{1}{N_{\text{ch}}} \sum_{j=1}^{N_{\text{ch}}} [N_{\text{eve}}(N_{\text{eve}} - 1)Q_j^2 + N_{\text{eve}}Q_j] - \mu_1^2 \\ &\approx \frac{N_{\text{eve}}^2}{N_{\text{ch}}} \sum_{j=1}^{N_{\text{ch}}} \sum_{i,i'=1}^{N_{\text{path}}} W_i P_j(E_i) W_{i'} P_j(E_{i'}) - \frac{N_{\text{eve}}^2}{N_{\text{ch}}} + \mu_1. \end{aligned} \quad (2)$$

This expression for μ_2 contains detailed information on the structure of the states of the nucleus in question. However, for a decay passing through many excited states, the focus shifts to average properties of the nuclear spectrum. In this perspective, the selection of energies and strengths by a particular nucleus is viewed as a realization, or sample [10], of a random distribution.

Two different scenarios for the random distribution underlying the realizations will be considered, corresponding to regular rotational bands and strongly interacting

bands, respectively. For regular bands, it will be assumed that the transition energies at angular momentum l as well as the band moment of inertia are independent random variables, which are selected from a distribution having a certain width about the average. For the strongly interacting bands, a random matrix model is assumed, resulting in a smooth spectrum and in considerable fluctuations in the transition probabilities [10] (Porter-Thomas fluctuations).

For random transition energies, the average over realizations picks out the diagonal part $i=i'$ of the double sum in Eq. (2). The result

$$\mu_2 \approx N_{\text{eve}}^2 P^{(2)} \sum_i^{N_{\text{path}}} W_i^2 + \mu_1 \quad (3)$$

is expressed through the second ($n=2$) moment of the recording probabilities $P^{(n)} = \int [P_j(E)]^n dE / \int dE$. The expression (3) for μ_2 contains the main terms, provided that $N_{\text{eve}} \gg 1$ and $P^{(2)} \gg (P^{(1)})^2$. Inserting $P^{(1)} = 1/N_{\text{ch}}$, and defining the effective number of paths

$$N_{\text{path}}^{(2)} \equiv \left(\sum_{i=1}^{N_{\text{path}}} W_i^2 \right)^{-1}, \quad (4)$$

Eq. (3) can be rewritten as

$$N_{\text{path}}^{(2)} = \frac{P^{(2)}}{P^{(1)}} \frac{N_{\text{eve}}}{\mu_2/\mu_1 - 1}. \quad (5)$$

For Porter-Thomas fluctuations, the average over realization picks out, first, identical paths, $i=i'$, for which $\langle W_i^2 \rangle = 9\langle W_i \rangle^2$, and, second, paths which have one transition in common, for which $\langle W_i W_{i'} \rangle = 3\langle W_i \rangle \langle W_{i'} \rangle$ [10]. The double sum over such two-dimensional paths results in a single sum over the single transition, which defines a one-dimensional path, with the probability denoted by w_i . Equation (5) can still be used, but now the effective number of paths is given by

$$N_{\text{path,PT}}^{(2)} = \left[\frac{4}{N_{\text{path}}^{(2)}} + 4 \frac{(p^{(1)})^2}{p^{(2)}} \frac{1}{n_{\text{path}}^{(2)}} \right]^{-1}. \quad (6)$$

Here $p^{(1)}$ and $p^{(2)}$ refer to one-dimensional channels, and the number of two-step paths $N_{\text{path}}^{(2)}$ and one-step paths $n_{\text{path}}^{(2)}$ are defined by Eq. (4), replacing W_i by the average transition probabilities $\langle W_i \rangle$ and $\langle w_i \rangle$, respectively.

The effective number of paths $N_{\text{path}}^{(2)}$ is defined to coincide with the actual number of paths in the case of equal probabilities, $W_i = 1/N_{\text{path}}$. For rotational decay through excited states, models for undamped and damped decay are used to obtain the probabilities, and thereby the number of paths. This number is then to be confronted with the empirical number of paths, given by the right-hand side of Eq. (5).

A program STATFIT has been developed to extract from the experimental data the values of μ_1 and μ_2 . In the analysis of the two-dimensional E_{γ_1} - E_{γ_2} spectrum, the

program makes a sweep through all data points $N(x,y)$ contained in the selected energy window and calculates a set of new spectra with the values μ_1, μ_2 for each point (x_0, y_0) according to the following equation:

$$\mu_i(x_0, y_0) = \frac{1}{N_{ch}(x,y)} \sum A_i(x,y) f(x-x_0, y-y_0). \quad (7)$$

Here $A_i(x,y)$ is equal to $N(x,y)$ for $i=1$ and is equal to $[N(x,y) - N_{FIT}(x,y)]^2$ for $i=2$, $f(x-x_0, y-y_0)$ is a Gaussian weighting function centered around (x_0, y_0) [normalized so that $\sum_{x,y} f(x-x_0, y-y_0) = 1$], with width σ , and the smooth reference spectrum $N_{FIT}(x,y)$ is calculated making use of a polynomial fit to the data points contained in a square surrounding each point (x,y) . The fitting and the evaluation procedure have been tested by varying the channel width, the size of the square, the order of the polynomial, and the width of the Gaussian smearing. It was found that a channel width of 4 keV, a square size of 7×7 channels, a third-order polynomial, and $\sigma = 1.9 \times 4$ keV represent a reasonable choice of the different parameters, providing a sensible compromise between selectivity, statistics, and smoothness for the analysis of the data.

It is known that the 2D raw spectra are dominated by intense stripes arising from coincidences with Compton-scattered photons. Such stripes would disturb the analysis significantly. The so-called COR treatment [11], where the COR spectrum is made from subtracting an uncorrelated average spectrum, UNCOR, from the raw spectrum, can eliminate a major part of this problem, almost without loss of statistics [7]. The COR treatment has been further improved by a minimization procedure, making use of the fluctuation analysis techniques [9].

After the improved COR treatment is performed, the peaks associated with known discrete lines are subtracted out, so that the value obtained for the effective number of paths will not be dominated by their large probabilities. The moments μ_1 and μ_2 as a function of E_{γ_1} and E_{γ_2} are then extracted from the modified experimental spectrum according to Eq. (7). In Fig. 2 examples of the various steps of the statistical analysis for the set of data [12] associated with the γ decay in $^{167,168}\text{Yb}$ are displayed. The data have been taken with the multidetector system ESSA30.

It is seen that the ridges become strongly magnified in the fluctuation spectrum μ_2/μ_1 , as compared to the COR spectrum. This result demonstrates that the ridge structures originate from the cold system, with low level density.

Making use of Eq. (5) the effective number of paths $N_{path}^{(2)}$ has been extracted by integrating the ridge in both the μ_1 and μ_2 spectra [9], and is displayed in the lower part of Fig. 3. A typical value $N_{path}^{(2)} = 30$ is found. For discrete rotational bands, the paths consist of transitions along the bands, and the theoretical value of $N_{path}^{(2)}$ is obtained by summing over bands up to the borderline ener-

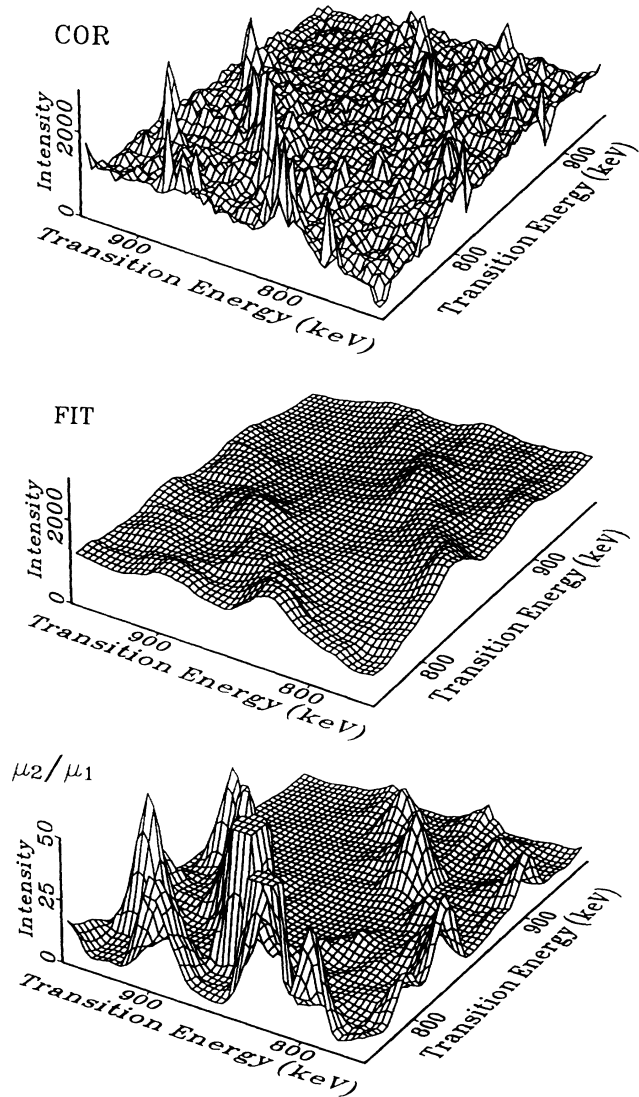


FIG. 2. Two-dimensional spectrum associated with coincidence measurements of the decay of $^{167,168}\text{Yb}$ for the COR=RAW-UNCOR and for the total average FIT. Also shown is the spectrum of fluctuations resulting from the ratio μ_2/μ_1 between the second and the first moment extracted from the data according to Eq. (7). The known discrete transitions have been removed from the right-hand side of the central valley.

gy U_0 :

$$\sum_{i=1}^{N_{path}} w_i^2 = \int_0^{U_0} \rho(U) [F(U)]^2 dU. \quad (8)$$

Here $\rho(U)$ is the level density [13] of both parities and signatures and $F(U)$ is the accumulated feeding function for populating a rotational band of energy U , determined from simulations [9]. Also shown in the figure is the number of levels N_{lev} obtained by integrating the level density from 0 to U_0 . It is seen that the best agreement

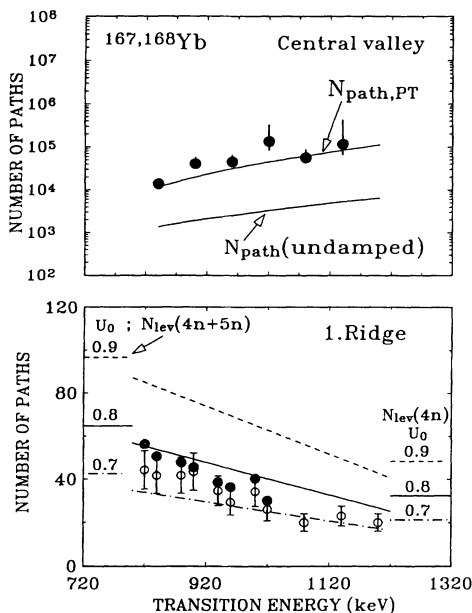


FIG. 3. The empirically determined values $N_{\text{path}}^{(2)}$. In the upper part, the values of N_{path} associated with coincidences with energies $E_{\gamma_1} = E_{\gamma_2}$ (valley) are shown. In the lower part, the corresponding results associated with the first ridge are plotted with open circles. Shown by solid circles is the result obtained by adding the number of removed discrete peaks to the value of $N_{\text{path}}^{(2)}$. Theoretical calculations carried out making use of Eq. (8) and of different values for U_0 are shown. Equal composition of intensity from the $4n$ and $5n$ reaction channels has been assumed for the lower transition energies, with a linear decrease of the $5n$ component up to 1200 keV. Also shown is the actual number of levels N_{lev} below U_0 , obtained by integrating the level density up to U_0 .

with the data is obtained using a value of U_0 between 700 and 800 keV for the case of $^{167,168}\text{Yb}$.

In contrast to the large fluctuations observed in the counting rate along the ridge structures, the region along the valley displays very small fluctuations as seen in the function μ_2/μ_1 displayed in Fig. 2. For the valley region the number of paths, determined through Eq. (5), is of the order of 10^5 , as shown in the upper part of Fig. 3. If the valley counts were produced by transitions along undamped bands with wildly fluctuating moments of inertia, Eq. (8) should still be applied, with the integration over U extending from U_0 to ∞ . This gives a value of $N_{\text{path}}^{(2)}$

which is an order of magnitude smaller than the empirical value. Also shown in Fig. 3 is the result of a calculation of $N_{\text{path,PT}}$, carried out assuming a rotational damping width [2,4,11] of 100 keV and the same level density parameter $a \approx 16 \text{ MeV}^{-1}$. It provides an overall account of the experimental findings.

We conclude that the fluctuation spectrum associated with the quasicontinuum γ decay displays a much more pronounced ridge-valley structure than the original spectrum, making it a powerful tool to study the structure of excited nuclei at high spin. One can divide the spectrum of $^{167,168}\text{Yb}$ into a low-energy region, as measured from the yrast line, where about 30 rotational bands are found, with very little branching among them, and a high-energy region where the stretched quadrupole decay has to be described in terms of a strength function, and where the number of paths is of the order of 10^5 . The dividing energy is found to be $U_0 \approx 750 \text{ keV}$.

The work has been supported by the Danish Natural Science Research Council.

- [1] G. A. Leander, Phys. Rev. C **25**, 2780 (1982).
- [2] J. C. Bacelar *et al.*, Phys. Rev. Lett. **55**, 1858 (1985).
- [3] F. S. Stephens *et al.*, Nucl. Phys. **A447**, 217c (1986); J. E. Draper *et al.*, Phys. Rev. Lett. **56**, 309 (1986).
- [4] B. Lauritzen *et al.*, Nucl. Phys. **A457**, 61 (1986).
- [5] R. A. Broglia *et al.*, Phys. Rev. Lett. **58**, 326 (1987).
- [6] F. S. Stephens, in *Proceedings of the Conference on High-Spin Nuclear Structure and Novel Nuclear Shapes, Argonne, Illinois, 1988* (ANL Report No. ANL-PHY-88-2).
- [7] B. Herskind *et al.*, in *Proceedings of the Third International Spring Seminar on Nuclear Physics, Ischia, Italy*, edited by A. Covello (World Scientific, Singapore, 1990).
- [8] B. Herskind *et al.*, Nucl. Phys. **A520**, 539c (1990).
- [9] B. Herskind *et al.*, in *Proceedings of the International School of Nuclear Physics, Erice, 1991*, edited by A. Faessler (to be published).
- [10] P. G. Hansen *et al.*, Nucl. Phys. **A518**, 13 (1990).
- [11] B. Herskind, in *Proceedings of the LXXXVII Varenna International School of Physics*, edited by L. Moretto and R. A. Ricci (North-Holland, Amsterdam, 1984).
- [12] J. Lisle *et al.*, Daresbury Annual report, 1987; (to be published).
- [13] Sven Åberg, Nucl. Phys. **A477**, 18 (1988).